LINES ON $K3$-QUARTICS VIA TRIANGULAR SETS

ALEX DEGTYAREV AND SŁAWOMIR RAMS

ABSTRACT. We prove the sharp upper bound of at most 52 lines on a complex $K3$-surface of degree 4 with a non-empty singular locus. We also classify the configurations of more than 48 lines on smooth complex quartics.

1. INTRODUCTION

Our main goal is to present an approach to study large line configurations on complex projective $K3$-quartics. In particular, we prove the following theorem.

Theorem 1.1 (see §7.2). *Let $X_4 \subset \mathbb{P}^3(\mathbb{C})$ be a degree 4 $K3$-surface with non-empty singular locus. Then X_4 contains at most 52 lines. Moreover, each $K3$-quartic with at least 49 lines contains four coplanar lines.*

The above bound is sharp: the existence of a complex $K3$-quartic with 52 lines and non-empty singular locus (two simple nodes) was shown by the first named author in 2016 (*via* Torelli's theorem, see [6, Theorem 1.10]) and the equation of the surface in question was found by D. Veniani, see [25, Example 5.5].

We conjecture that the quartic surface discovered in [6, Theorem 1.10] is the only quartic that attains the bound of Theorem 1.1, but the proof of this fact is beyond the scope of this paper.

It is well-known that the complexity of large line configurations on projective $K3$-surfaces decreases as the degree d of the polarization grows. In particular, a complete classification of close to maximal configurations is known for octics (see [2, Theorem 1.1]) and sextics (to appear in [3]): the respective upper bounds are 32 and 36 in the presence of a singularity *vs.* 36 and 42 in the smooth case. In contrast, even though quartic surfaces with singular points have been a subject of intensive study ever since the 19-th century (see, *e.g.*, the classical treatise [12]), hardly anything is known about large line configurations on such surfaces. The main reason is the existence of the so-called *triangular* configurations on quartics (see §2.4 for the definition) — a property that drastically increases the complexity of the problem. Here, we circumvent this difficulty with the help of the so-called *triangular sets* introduced in §3.

One can easily check that the degree-d Fermat surface (over $\mathbb{C}$) contains exactly $3d^2$ lines for $d > 2$. Moreover, for almost all integers d the Fermat surface is the best known example of a smooth complex projective surface with many lines, and the question whether smooth degree-d surfaces with more lines exist remains open. To illustrate the power of our approach, we refine the results of [8] and classify

TABLE 1. Smooth complex quartics with at least 49 lines

Γ	$|\mathrm{Aut}\,\Gamma|$	$|\mathrm{Sym}\,X_4|$	(r,c)	$\mathrm{NS}(X_4)^\perp$
$\mathbf{X}_{64}$	4608	$(192, 1493)^6$	$(1,0)$	$[8,4,8]$
$\mathbf{X}'_{60}$	480	$(60,5)^2$	$(1,0)$	$[4,2,16]$
$\mathbf{X}''_{60}$	240	$(60,5)^2$	$(0,1)$	$[4,1,14]$
$\mathbf{X}_{56}$	128	$(16,11)^4$	$(0,1)$	$[8,0,8]$
$\mathbf{Y}_{56}$	64	$(16,8)^2$	$(1,0)$	$^*[2,0,32]$
$\mathbf{Q}_{56}$	384	$(48,50)^2$	$(1,0)$	$[4,2,16]$
$\mathbf{X}_{54}$	384	$(24,12)^2$	$(1,0)$	$[4,0,24]$
$\mathbf{Q}_{54}$	48	$(8,5)$	$(1,0)$	$[4,2,20]$
$\mathbf{X}'_{52}$	24	$(3,1)$	$(1,0)$	$[8,4,12]$
$\mathbf{X}''_{52}$	36	$(6,1)$	$(1,0)$	$[4,2,20]$
$\mathbf{X}'''_{52}$	320	$(20,3)^4$	$(1,0)$	$[10,0,10]$
$\mathbf{X}^{\mathrm{v}}_{52}$	32	$(4,1)^2$	$(1,0)$	$[10,4,10]$
$\mathbf{Y}'_{52}$	8	$(4,1)^2$	$(1,0)$	$^*[2,0,38]$
			$(0,1)$	$[8,2,10]$
$\mathbf{Y}''_{52}$	8	$(4,2)^2$	$(1,0)$	$^*[2,1,40]$
			$(0,1)$	$[4,1,20]$
			$(0,1)$	$[8,1,10]$
$\mathbf{Z}_{52}$	384	$(12,3)^2$	$(1,0)$	$^*\mathbf{U}(2)\oplus[24]$
(52)	384	$(8,5)$	$(1,0)$	$[-8]\oplus[4,2,4]$
$\mathbf{Q}'_{52}$	64	$(8,5)$	$(1,0)$	$[4,0,24]$
$\mathbf{Q}''_{52}$	64	$(16,11)$	$(0,1)$	$[8,4,12]$
$\mathbf{Q}'''_{52}$	96	$(4,1)^6$	$(1,0)$	$[10,5,10]$
$\mathbf{X}_{51}$	12	$(6,1)$	$(0,1)$	$[4,1,22]$
			$(1,0)$	$[6,3,16]$
$\mathbf{X}'_{50}$	18	$(3,1)$	$(1,0)$	$[4,2,28]$
$\mathbf{X}''_{50}$	12	$(3,1)$	$(2,0)$	$[4,0,24]$
$\mathbf{X}'''_{50}$	16	$(2,1)^2$	$(0,1)$	$[4,0,24]$
$\mathbf{Z}_{50}$	160	$(10,1)^2$	$(1,0)$	$\mathbf{U}(5)\oplus[4]$
(50)	96	$(8,5)$	$(1,0)$	$^*\mathbf{U}(2)\oplus[28]$
$\mathbf{Z}_{49}$	36	$(3,1)$	$(1,0)$	$^*\mathbf{U}(2)\oplus[28]$

all configurations of at least 49 lines on *smooth* quartics (*i.e.*, the configurations that are larger than the one on the Fermat quartic). Remarkably, compared to [8], we found but three new configurations: one of rank 20 ($\mathbf{Q}'''_{52}$ previously found in [6]) and two of rank 19 (designated as (52) and (50) in Table 1). On the other hand, there are at least 28 configurations of 48 lines on smooth quartics, giving yet another reason why 48 is a reasonable threshold (*cf.* also Proposition 5.6 and Remark 4.11 below).

Theorem 1.2 (see §7.3)**.** *Up to isomorphism, there are* 26 *configurations of at least* 49 *lines on smooth quartic surfaces, see Table 1. They are realized by* 34 *singular* (aka *projectively rigid*) *surfaces* (18 *real and* 8 *pairs of complex conjugate*) *and five connected* 1*-parameter families.*

As a consequence, we answer a question left open in [8, Addendum 1.4].

Addendum 1.3 (see §7.4)**.** *The complete list of values taken by the number of* real *lines on a* real *smooth quartic is*

$$\{0, 1, \ldots, 49, 50, 52, 56\}.$$

The configurations of more than 48 *real lines on a real smooth quartic are those marked with a* * *in* Table 1.

Listed in Table 1 are:
- the name of the configuration Γ (mostly following [8]); the subscript always refers to the number of lines (vertices of Γ);
- the size of the group $\operatorname{Aut}\Gamma$ of abstract graph automorphisms of Γ;
- the group $\operatorname{Sym} X_4$ of simplectic automorphisms of a generic quartic X_4 with the given Fano graph, in the form (size, index), referring to the `SmallGroup` library in `GAP` [9]; the superscript is the index of $\operatorname{Sym} X_4$ in the full group $\operatorname{Aut}(X_4, h)$ of projective automorphisms of X_4 (if greater than 1);
- the numbers (r, c) of, respectively, real and pairs of complex conjugate components of the equilinear moduli space;
- the (generic, if $\operatorname{rk} \geqslant 3$) transcendental lattice $T := \operatorname{NS}(X_4)^\perp$; it is marked with a * if the corresponding deformation family has a real quartic with all lines real (see [8, Lemma 3.8]).

If T is not determined by Γ, each lattice is listed in a separate row (following the main entry), and the numbers (r, c) of components are itemized accordingly.

As in [5], we use the following notation for common integral lattices:
- $[a] := \mathbb{Z}u$ is the lattice of rank 1 given by the condition $u^2 = a$;
- $[a, b, c] := \mathbb{Z}u + \mathbb{Z}v$, $u^2 = a$, $u \cdot v = b$, $v^2 = c$, is a lattice of rank 2; when it is positive definite, we assume that $0 < a \leqslant c$ and $0 \leqslant 2b \leqslant a$: then, u is a shortest vector, v is a next shortest one, and the triple (a, b, c) is unique;
- $\mathbf{U} := [0, 1, 0]$ is the unimodular even lattice of rank 2;
- $L(n)$ denotes the lattice obtained by the scaling of a given lattice L by a fixed integer $n \in \mathbb{Z}$.

In general, we maintain the standard notation for various objects associated to a lattice L (the determinant, discriminant group, *etc.*) —see, *e.g.*, [1, 16]. The inertia indices of the quadratic form $L \otimes \mathbb{R}$ are denoted by $\sigma_{\pm,0}(L)$.

1.1. **Contents of the paper.** Roughly, the paper consists of two parts: the discrete one (§2–§6) and the geometric one (§7).

Our approach is a refinement of the technique developed in [8, 2], and we recall the necessary facts and introduce certain technical terms (*e.g.*, acceptable graphs) in §2. Then, in §3, we define the main technical tool, *viz.* the triangular set, and discuss methods of extending a given graph by a collection of triangular sets. Finally, after those preparations, we present the proof of Proposition 3.12, which is the discrete counterpart of the most difficult case of Theorem 1.1.

§4 is a digression: we restrict our attention to the case of smooth lattices (*i.e.*, we assume that the lattice contains no exceptional divisors) and apply triangular sets to classify geometric Fano graphs with at least 49 vertices.

In §5 and §6, we turn back to the general case (with exceptional divisors allowed) and study the properties of triangular free Fano graphs.

Finally, in §7 we recall the definition of the Fano graph (resp. extended Fano graph) of a surface and its relation to the geometricity of the Fano graph of a

lattice, see Theorem 7.4 (resp. Theorem 7.7) and prove the principal results of the paper, *viz.* Theorem 1.1 and Theorem 1.2.

1.2. **History of the problem.** As mentioned, configurations of lines (or, more generally, smooth rational curves) on quartic surfaces in $\mathbb{P}^3$ have been a subject of intensive study ever since the 19-th century. Still, the methods of Italian school were not efficient enough to deal with the classification of large line configurations on such surfaces. It was not until the last decade that the theory of elliptic fibrations, Mordell–Weil groups, Torelli's theorem and progress in algorithmic methods in the theory of lattices led to a substantial progress in the case of smooth quartics: sharp bound for the number of lines over fields of characteristic $p \neq 2, 3$ (see [20, 18, 8]), $p = 3$ (see [17]), $p = 2$ (see [7]), the classification of large configurations (see [8]), explicit equations of surfaces with many lines (see [24] and the bibliography therein). Strangely enough, the Bogomolov–Miyaoka–Yau inequality yields no bounds in the case of quartics (see [14]).

In contrast, in spite of long interest (see, *e.g.*, the classical text [12]), far less is known in the case of quartic surfaces with singular points — essentially, it was only shown that, over a field of characteristic $p \neq 2$, the number of lines on a quartic with singularities cannot exceed the maximal number of lines on a smooth quartics — see [23, 25, 11]. For $p = 2$ the maximal number of lines on a quartic with singularities is 68 (*vs.* 60 in the smooth case, see [22]) and we do know projective models of surfaces that attain this maximum (see [17]).

A refinement of the method pioneered in [8] led to the complete picture of large line configurations on smooth degree-d $K3$-surfaces for $d > 2$ in [5]. Vinberg's algorithms combined with the above methods yield a means to classify the large configurations of lines on degree-d $K3$-surfaces with at worst Du Val singularities for $d > 4$ (see [2, 3]). The methods of [2] are not sufficient to deal with the case of quartics (*i.e.*, $d = 4$): the existence of triangles (*i.e.*, $\tilde{\mathbf{A}}_2$-configurations) of lines and the fact that, on quartic surfaces, said triangles may interlace lead to numerous configurations that are excluded on degree-d $K3$-surfaces for $d > 4$. In the present paper, we discuss an approach to deal with such configurations. However, in order to keep our exposition compact, we apply our method to find the maximal number of lines on a complex $K3$-quartics with non-empty singular locus, but we do not try to classify all configurations of 52 lines.

1.3. **Acknowledgements.** This paper was mostly written during our research stay at the *Max-Planck-Institut für Mathematik*, Bonn. We are grateful to MPIM for creating perfect working conditions. S.R. thanks IM PAN (Cracow, Poland) for the support that enabled him to complete this project.

2. Preliminaries

In this section we recall the main technical tools that we use in our work. To shorten the exposition, we focus on the case of 4-polarized 2-admissible lattices and graphs. The details and more general statements can be found in [2]. To keep the exposition continuous,we assume the reader familiar with the basics of the theory of $K3$-surfaces, (-2)-curves, *etc.* and adopt a formal graph-theoretical language. The relation of graphs considered in §2–§6 to the problem at hand, *i.e.*, lines on quartic surfaces, is briefly discussed in §7.1 below, right before the proofs of the principal results of the paper.

2.1. **Polarized lattices.** Recall that a nondegenerate lattice S is called *hyperbolic* if $\sigma_+ S = 1$. A *polarized lattice* $S \ni h$ is a hyperbolic lattice S equipped with a distinguished vector h of positive square; the square h^2 is called the *degree* of the polarization and S is said to be h^2-polarized. Here we assume $h^2 = 4$, so whenever we speak of a *polarized lattice* we mean a 4-*polarized lattice*. Furthermore, we confine ourselves to lines and exceptional divisors (resp. only lines in §4), leaving out smooth rational curves of higher degree.

Remark 2.1. We make frequent use of the following obvious observation: if S is a hyperbolic lattice, then any sublattice $N \subset S$ is either semidefinite (and then one has $\operatorname{rk} \ker N = 1$) or nondegenerate.

For a polarized lattice and $n = 0, 1$, one defines the sets

$$\operatorname{root}_n(S, h) := \big\{ r \in S \mid r^2 = -2,\, r \cdot h = n \big\}.$$

As in [2, §2.2], we put $\mathfrak{rt}(S, h) \subset h^\perp \subset S$ (resp. $\mathcal{C}^+(S, h)$) to denote the sublattice generated by $\operatorname{root}_0(S, h)$ (resp. the positive cone). Recall that every connected component $\Delta^\sharp$ of

$$\mathcal{C}^+(S, h) \smallsetminus \bigcup_{r^2 = -2} r^\perp$$

is a *fundamental polyhedron* for the group generated by reflections of S.

By definition, $\mathfrak{rt}(S, h)$ is a root lattice and each fixed Weyl chamber Δ for (the group generated by reflections of) $\mathfrak{rt}(S, h)$ gives rise to a distinguished fundamental polyhedron $\Delta^\sharp$. We put $\{\Delta\}$ to denote the "outward" roots orthogonal to the walls of Δ and define the (plain) *Fano graph* of the polarized lattice (S, h) with a distinguished Weyl chamber Δ for $\mathfrak{rt}(S, h)$ as the set of vertices

$$(2.2) \qquad \operatorname{Fn}_\Delta(S, h) := \{\Delta^\sharp\}_1 := \big\{ l \in \operatorname{root}_1(S, h) \mid l \cdot e \geqslant 0 \text{ for all } e \in \{\Delta\} \big\},$$

with two vertices $l_1 \neq l_2$ connected by an edge of multiplicity $l_1 \cdot l_2$. The bi-colored *extended Fano graph* is defined as

$$(2.3) \qquad\qquad \operatorname{Fn}_\Delta^{\mathrm{ex}}(S, h) := \{\Delta^\sharp\}_1 \cup \{\Delta\},$$

with the same convention about the multiplicities of the edges and vertices v colored according to the value $v \cdot h \in \{0, 1\}$.

Definition 2.4. Let $S \ni h$ be a polarized lattice and let Γ be a subset of $\operatorname{root}_1(S, h)$.

    (1) A Weyl chamber Δ is called *compatible* with Γ if $\Gamma \subset \operatorname{Fn}_\Delta(S, h)$.

    (2) A root $r \in \operatorname{root}_0(S, h)$ is called *separating* with respect to Γ if there is a pair of vertices $u, v \in \Gamma$ *separated* by r, so that $r \cdot u > 0$ and $r \cdot v < 0$.

Finally, in order to use general theory of $K3$-surfaces in the sequel we need the following definition.

Definition 2.5. A polarized lattice $S \ni h$ is called:

    (1) *admissible*, if there is no vector $p \in S$ such that $p^2 = 0$ and $p \cdot h = 2$;

    (2) *geometric*, if it is admissible and there exists a primitive isometry

$$S \hookrightarrow \mathbf{L} := 2\mathbf{E}_8 \oplus 3\mathbf{U}.$$

2.2. **Subgeometric and geometric graphs.** Let Γ be a (plain) graph. To Γ we associate the polarized lattice

$$(2.6) \qquad \mathcal{F}(\Gamma) := (\mathbb{Z}\Gamma + \mathbb{Z}h)/\ker, \qquad h^2 = 4, \quad h \cdot v = 1 \text{ for } v \in \Gamma.$$

where $\mathbb{Z}\Gamma$ is the lattice freely generated by the vertices $v \in \Gamma$, so that $u \cdot v = n$ when $u \ne v$ are connected by an n-fold edge, and $v^2 = -2$ for each $v \in \Gamma$.

Convention 2.7. As in [2, §4], we speak of *polarized* graphs Γ (omitting the degree which is fixed to equal 4), and we apply to Γ the lattice theoretic terminology such as the *rank* $\operatorname{rk}\Gamma := \operatorname{rk}\mathcal{F}(\Gamma)$ *etc.* Furthermore, we treat the vertices of Γ as vectors in $\mathcal{F}(\Gamma)$: *e.g.*, $u \cdot v \in \mathbb{Z}$ stands for the multiplicity of the edge $[u, v]$, and we say that $u, v \in \Gamma$ *intersect* if $u \cdot v = 1$. The only exception from this rule is the classification of graphs according to the inertia indices of $\mathbb{Z}\Gamma$ rather than $\mathcal{F}(\Gamma)$ (which is *always* assumed hyperbolic): thus, we say that Γ is

- *elliptic*, if $\sigma_+(\mathbb{Z}\Gamma) = \sigma_0(\mathbb{Z}\Gamma) = 0$,
- *parabolic*, if $\sigma_+(\mathbb{Z}\Gamma) = 0$ and $\sigma_0(\mathbb{Z}\Gamma) > 0$, and
- *hyperbolic*, if $\sigma_+(\mathbb{Z}\Gamma) = 1$ (no assumption on σ_0).

Recall that any connected elliptic (resp. parabolic) graph is a Dynkin diagram (resp. affine Dynkin diagram); as in [5], we order the isomorphism classes of affine Dynkin diagrams according to their Milnor number, followed by $\mathbf{A} < \mathbf{D} < \mathbf{E}$. Recall also that, for each connected parabolic subgraph Σ, there is a unique positive minimal generator $\kappa_\Sigma \in \ker \mathbb{Z}\Sigma$; it has the form $\kappa_\Sigma = \sum m_c c$, $c \in \Sigma$, with all $m_c > 0$.

We define the *perturbation order* on the set of (isomorphism classes of) elliptic and parabolic graphs: $\Gamma' \lhd \Gamma''$ if Γ' is isomorphic to an induced subgraph of Γ''.

Given an isotropic subgroup $\mathcal{K} \subset \operatorname{discr}\mathcal{F}(\Gamma)$ (*aka* kernel), we consider the finite index extension $\mathcal{F}(\Gamma, \mathcal{K})$ of $\mathcal{F}(\Gamma)$ by $\mathcal{K}$ (*cf.* [16]). The pair $(\Gamma, \mathcal{K})$ is said to be *extensible* if it admits a compatible Weyl chamber Δ for $\mathfrak{rt}(\mathcal{F}(\Gamma, \mathcal{K}), h)$ (see Definition 2.4):

$$\Gamma \subset \operatorname{Fn}_\Delta \mathcal{F}(\Gamma, \mathcal{K}).$$

Recall that, by [2, Lemma 3.4], we have

$$(2.8) \qquad (\Gamma, \mathcal{K}) \text{ is extensible if and only if } \mathcal{F}(\Gamma, \mathcal{K}) \text{ has no separating roots}$$

(see Definition 2.4); moreover, if this is the case, the compatible Weyl chamber $\Delta \subset \mathfrak{rt}\,\mathcal{F}(\Gamma, \mathcal{K})$ is unique. Therefore, for an extensible pair $(\Gamma, \mathcal{K})$ one can define its *saturation* and *extended saturation*

$$\operatorname{sat}(\Gamma, \mathcal{K}) := \operatorname{Fn}_\Delta \mathcal{F}(\Gamma, \mathcal{K}), \qquad \operatorname{sat}^{\mathrm{ex}}(\Gamma, \mathcal{K}) := \operatorname{Fn}_\Delta^{\mathrm{ex}} \mathcal{F}(\Gamma, \mathcal{K}).$$

A graph Γ (resp. pair $(\Gamma, \mathcal{K})$) is called *admissible* if it is extensible and the lattice $\mathcal{F}(\Gamma)$ (resp. $\mathcal{F}(\Gamma, \mathcal{K})$) is admissible. Then, an isotropic subgroup $\mathcal{K} \subset \operatorname{discr}\mathcal{F}(\Gamma)$ is called a *geometric kernel* if the lattice $\mathcal{F}(\Gamma, \mathcal{K})$ is geometric. We follow [2] and put

$$\mathfrak{G}(\Gamma) := \big\{ \mathcal{K} \subset \operatorname{discr}\mathcal{F}(\Gamma) \ \big| \ \mathcal{K} \text{ is geometric}\big\}.$$

After those preparations we can recall the following definition.

Definition 2.9. Let Γ be a graph.
1. We call Γ *subgeometric* if the set $\mathfrak{G}(\Gamma)$ is non-empty.
2. A subgeometric graph Γ is called *geometric* if $\Gamma \cong \operatorname{sat}(\Gamma, \mathcal{K})$ for a certain kernel $\mathcal{K} \in \mathfrak{G}(\Gamma')$.
3. A *bi-colored* graph Γ' is *geometric* if $\Gamma' \cong \operatorname{Fn}_\Delta^{\mathrm{ex}}(S, h)$ for some geometric polarized lattice $S \ni h$.

2.3. **Algorithms.** In many arguments we use computer-aided test to check that a given graph satisfies certain conditions. All algorithms are found in [2, Appendix]. Given a graph Γ, one can check whether:

(1) $\mathcal{F}(\Gamma)$ is hyperbolic, *i.e.*, $\sigma_+\mathcal{F}(\Gamma) = 1$; straight as it is, this can often be done fast in bulk, see [2, Lemmas A.3, A.4];

(2) Γ is extensible and admissible, see the master test in [2, §A.1.1];

(3) Γ is (sub-)geometric, see [2, §A.1.2].

The principal tool of [2] was starting from a sufficiently large initial graph Γ_0 and extending it by adding one vertex at a time, see §A.4 in *loc. cit.* This is what is done in this paper, too, see §5 and §6, where, without much explanation, we merely state the updated results. The principal novelty of this paper is §3, where, due to the more complicated geometric nature of the problem, extra vertices have to be added in groups of up to three. The details are discussed in §3.3.

Remark 2.10. A technical, but crucial part of our (as well as any lattice-based) approach is the fact that a geometric graph Γ has $\mathrm{rk}\,\Gamma \leqslant 20$. It follows that, if $\mathrm{rk}\,\Gamma' = 20$, any geometric overgraph $\Gamma \supset \Gamma'$ would be of the form $\mathrm{sat}(\Gamma', \mathcal{K})$ for some $\mathcal{K} \in \mathfrak{G}(\Gamma')$, and all such finite index extensions of $\mathcal{F}(\Gamma')$ can easily be found using [16] (see the *saturation lists* in [2, §A.1.3]). Therefore, we introduce another technical term:

$$\Gamma \text{ is } \textit{acceptable} \text{ if it is subgeometric and } \mathrm{rk}\,\Gamma \leqslant 19.$$

It is understood that, after each step of every algorithm, only *acceptable* graphs are left for the further processing (and, thus, we do not need to add dozens of vertices to reach line counts over 50), whereas each intermediate graph Γ of rank $\mathrm{rk}\,\Gamma = 20$ is excluded upon computing its saturation list and recording all "interesting" (*cf.* Remark 3.24 below) geometric overgraphs to a global master list.

2.4. **Classification of graphs in terms of girth.** Following [5, 8], we subdivide parabolic and hyperbolic graphs Γ according to the type of the minimal (in the sense of Convention 2.7) affine Dynkin diagram $\Sigma \subset \Gamma$. The most important classes can also be characterised in terms of the *girth* $\mathrm{girth}(\Gamma)$ (the length of a shortest cycle in Γ, with the convention that the girth of a forest is ∞). Thus, Γ is called

- *triangular*, or $\tilde{\mathbf{A}}_{2\text{-}}$, if $\mathrm{girth}(\Gamma) = 3$,
- *quadrangular*, or $\tilde{\mathbf{A}}_{3\text{-}}$, if $\mathrm{girth}(\Gamma) = 4$,
- *pentagonal*, or $\tilde{\mathbf{A}}_{4\text{-}}$, if $\mathrm{girth}(\Gamma) = 5$,
- *astral*, or $\tilde{\mathbf{D}}_{4\text{-}}$, if $\mathrm{girth}(\Gamma) \geqslant 6$ and Γ has a vertex of valency $\geqslant 4$.

All other graphs are *locally elliptic*, *i.e.*, one has $\mathrm{val}\,v \leqslant 3$ for each vertex $v \in \Gamma$ (and we assume $\mathrm{girth}(\Gamma) \geqslant 6$ to exclude a few trivial cases).

Given a graph Γ and a distinguished connected parabolic subgraph $\Sigma \subset \Gamma$, the *pencil* Π induced by Σ is defined as

$$(2.11) \qquad \Pi := \Pi(\Gamma \supset \Sigma) := \Sigma \cup \big\{ l \in \Gamma \mid l \cdot c = 0 \text{ for all vertices } c \in \Sigma \big\}.$$

This graph $\Pi \supset \Sigma$ is parabolic as it is orthogonal to κ_Σ (see Convention 2.7 and Remark 2.1). We have $\Gamma = \Pi \cup \sec^*$, where

$$(2.12) \qquad \sec^* := \sec^*(\Gamma \supset \Sigma) := \big\{ l \in \Gamma \smallsetminus \Sigma \mid l \cdot c = 1 \text{ for a vertex } c \in \Sigma \big\}.$$

The elements of $\sec^*$ are called the (*multi-*)*sections*, or *m-sections* of Π, where the integer $m := l \cdot \kappa_\Sigma$ is the *multiplicity* of a section l. If $m = 1$, the section is called

simple, otherwise, *multiple*. Fixing an order $\Sigma = (c_1, \ldots, c_n)$, we also consider

$$
\begin{aligned}
(2.13) \qquad \mathrm{sec}_i &:= \mathrm{sec}(\Gamma \supset \Sigma \ni c_i) \ := \big\{ l \in \Gamma \smallsetminus \Sigma \ \big| \ l \cdot c_j = \delta_{ij} \ \text{for} \ c_j \in \Sigma \big\}, \\
\mathrm{sec}_i^* &:= \mathrm{sec}^*(\Gamma \supset \Sigma \ni c_i) := \big\{ l \in \Gamma \smallsetminus \Sigma \ \big| \ l \cdot c_i = 1 \big\} \supset \mathrm{sec}_i,
\end{aligned}
$$

where $1 \leqslant i \leqslant n$ and δ_{ij} is the Kronecker symbol. We have

(2.14)   each set $\mathrm{sec}_i^* \supset \mathrm{sec}_i$, $i = 1, \ldots, n$, is either elliptic or parabolic,

as it is orthogonal to the isotropic vector $h - c_i \neq 0$ (see Remark 2.1).

In the future, we almost never use the correct, but long notation referring to the full flag, as $\Gamma \supset \Sigma = (c_1, \ldots, c_n)$ are always assumed fixed.

3. Triangular sets

A *triangular set*, or $\triangle$-*set*, is an induced subgraph of an admissible graph whose all connected components are of type $\tilde{\mathbf{A}}_2$, $\mathbf{A}_3$, $\mathbf{A}_2$, or $\mathbf{A}_1$. Clearly, each triangular pencil is a $\triangle$-set, but not *vice versa*: a $\triangle$-set may also be elliptic, *i.e.*, have no type $\tilde{\mathbf{A}}_2$ components. Combinatorially, a $\triangle$-set Θ is uniquely of the form

$$
(3.1) \qquad \tilde{a}_2 \tilde{\mathbf{A}}_2 \oplus a_3 \mathbf{A}_3 \oplus a_2 \mathbf{A}_2 \oplus a_1 \mathbf{A}_1, \qquad (\tilde{a}_2, a_3, a_2, a_1) \in \mathbb{N}^4,
$$

and the *coefficient quadruple* $(\tilde{a}_2, a_3, a_2, a_1)$ determines Θ up to isomorphism. The isomorphism classes of $\triangle$-sets (or coefficient quadruples) are called *patterns*.

We define the cardinality $|\theta|$ of a pattern θ as that of any of its representatives and introduce the following order on the set of patterns:

$$
(3.2) \qquad \theta' \prec \theta'' \quad \text{iff} \quad
\begin{cases}
|\theta'| < |\theta''| \ \text{or} \\
|\theta'| = |\theta''| \ \text{and} \ (\tilde{a}_2', a_3', a_2', a_1') > (\tilde{a}_2'', a_3'', a_2'', a_1''),
\end{cases}
$$

where the coefficient quadruples are compared lexicographically. (Pay attention to the *reverse* lexicographic order!) This order is not to be mixed with the perturbation order defined in Convention 2.7. The latter, for $\triangle$-sets, is easily described in terms of the coefficient quadruples: $\theta' \vartriangleleft \theta''$ if and only if $(\tilde{a}_2', a_3', a_2', a_1')$ is obtained from $(\tilde{a}_2'', a_3'', a_2'', a_1'')$ by a finite sequence of *elementary perturbations* of the form

$$
(\tilde{a}_2, a_3, a_2, a_1) \mapsto (\tilde{a}_2, a_3, a_2, a_1) + \delta,
$$
$$
\delta \in \big\{ (0, 0, -1, 1), (0, -1, 1, 0), (0, -1, 0, 2), (-1, 0, 1, 0) \big\}
$$

provided that, at each step, the quadruple remains in $\mathbb{N}^4$.

3.1. Constructing triangular graphs.

Let Γ be a triangular admissible graph, *cf.* §2.4. Fix a type $\tilde{\mathbf{A}}_2$ fiber $\Sigma = (c_1, c_2, c_3) \subset \Gamma$ and consider the pencil Π and sets sec_i, $i = 1, 2, 3$, see (2.11) and (2.13), respectively.

Lemma 3.3. *A triangular pencil Π has at most one multiple section*; *hence,*

$$
0 \leqslant |\Gamma| - |\Pi \cup \mathrm{sec}_1 \cup \mathrm{sec}_2 \cup \mathrm{sec}_3| \leqslant 1.
$$

Furthermore, if a multiple section s exists, it is disjoint from each sec_i, $i = 1, 2, 3$.

Proof. Consider a multiple section s and let $e := h - c_1 - c_2 - c_3 - s$.

If $s \cdot c_1 = s \cdot c_2 = s \cdot c_3 = 1$, then e is orthogonal to h and each c_i, $i = 1, 2, 3$. Hence, $e = 0$ (see Remark 2.1) and any other line l intersects exactly one of c_1, c_2, c_3, s, implying both statements.

Likewise, if $s \cdot c_1 = s \cdot c_2 = 1$ and $s \cdot c_3 = 0$, then e is an exceptional divisor and $e \cdot s = e \cdot c_3 = 1 > 0$. Hence, any other line l intersects *at most* one of c_1, c_2, c_3, s, as otherwise $l \cdot e < 0$ and e would separate s and l, see (2.8). $\qquad \square$

Lemma 3.4. *Each set* $\sec_i$, $i = 1, 2, 3$, *is a* $\triangle$-*set.*

Proof. In view of (2.14), it suffices to rule out the connected components of $\sec_i$ containing $\tilde{\mathbf{A}}_3$, $\mathbf{A}_4$, or $\mathbf{D}_4$. Each of the offending graphs has a chain
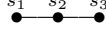
$$\overset{s_1}{\bullet}\!\!-\!\!\overset{s_2}{\bullet}\!\!-\!\!\overset{s_3}{\bullet}$$

and another vertex l adjacent to at least one of s_1, s_2, s_3. Then $s := s_1 + s_2 + s_3$ is a root, $s \cdot h = s \cdot c_i = 3$, and $l \cdot s > 0$; hence, $e := -h + c_i + s$ is an exceptional divisor separating s_1 and l, see (2.8). $\qquad \square$

Now, our goal is to describe all geometric graphs Γ of size $|\Gamma| \geqslant 53$. In view of Lemma 3.3, it suffices to consider trigonal pencils $\Sigma \subset \Pi \subset \Gamma$ such that

$$|\Pi| + |\sec_1| + |\sec_2| + |\sec_3| \geqslant 52.$$

Clearly, we can also assume that $\Pi \subset \Gamma$ is maximal with respect to (3.2) and the edges c_1, c_2, c_3 of Σ are ordered so that $\sec_1 \succcurlyeq \sec_2 \succcurlyeq \sec_3$. These assumptions give rise to the following *compatibility conditions* on the patterns $\pi \ni \Pi$ and $\theta_i \ni \sec_i$:

$$(3.5) \qquad \pi \vdash \theta_1 \quad \text{if} \quad 3|\theta_1| + |\pi| \geqslant 52 \text{ and } \big(\theta_1 \preccurlyeq \pi \text{ or } \theta_1 \text{ is elliptic}\big);$$

$$(3.6) \qquad (\pi \vdash \theta_1) \vdash \theta_2 \quad \text{if} \quad 2|\theta_2| + |\theta_1| + |\pi| \geqslant 52 \text{ and } \theta_2 \preccurlyeq \theta_1;$$

$$(3.7) \qquad (\pi \vdash \theta_1 \vdash \theta_2) \vdash \theta_3 \quad \text{if} \quad |\theta_3| + |\theta_2| + |\theta_1| + |\pi| \geqslant 52 \text{ and } \theta_3 \preccurlyeq \theta_2.$$

In (3.5), we assume one of the terms, π or θ_1, fixed and treat the condition as a restriction on the other term. The other two conditions are restrictions on the last term provided that the parenthesized part is fixed.

Since $\triangle$-sets appear as sets of sections, for an ordered fiber $\tilde{\mathbf{A}}_2 \cong \Sigma = (c_1, c_2, c_3)$ and $\triangle$-set Θ we define $\Sigma \sqcup_i \Theta$, where $i = 1, 2, 3$, as the graph obtained from the disjoint union of Σ and Θ by connecting c_i to each vertex $v \in \Theta$ by a simple edge.

This construction extends to patterns, producing an isomorphism class of graphs. Checking the parameter quadruples $(\tilde{a}_2, a_3, a_2, a_1)$ one-by-one, it is fairly easy to compute the sets of patterns

$$\mathcal{P} := \{\text{subgeometric triangular pencils}\}/\!\cong, \text{ and}$$

$$\mathcal{T} := \{\triangle\text{-sets } \Theta \text{ such that } \tilde{\mathbf{A}}_2 \sqcup_i \Theta \text{ is subgeometric}\}/\!\cong.$$

(To simplify the computation, for $\mathcal{P}$ one can start from Shimada's list [21] of Jacobian elliptic $K3$-surfaces, and for $\mathcal{T}$ one can take into account the bound $\operatorname{val} c_i \leqslant 20$ found in [23].) Then, condition (3.5) becomes a binary relation from $\mathcal{P}$ to $\mathcal{T}$. The other conditions also descend to patterns, as do the rank functions:

$$(3.8) \qquad \begin{aligned} \operatorname{rk}(\pi) &= |\Pi| - \tilde{a}_2(\Pi) + 2, \quad \Pi \in \pi \in \mathcal{P} \\ \operatorname{rk}(\tilde{\mathbf{A}}_2 \sqcup_i \theta) &= |\Theta| - \tilde{a}_2(\Theta) + 4, \quad \Theta \in \theta \in \mathcal{T}, \end{aligned}$$

where $\tilde{a}_2(\cdot)$ stands for the number of parabolic components.

The next lemma is an immediate consequence of this computation. For the last statement, we merely list all geometric extensions (*e.g.* using algorithms from [2, Appendix A]) of the four graphs of rank 18 or 19, see (3.8); in fact, the sharp bound in Lemma 3.9(3) is $|\Gamma| \leqslant 29$.

Lemma 3.9. *In a geometric graph* Γ, *for any type* $\tilde{\mathbf{A}}_2$ *fiber* Σ *one has*:

(1) $|\sec_i| \leqslant 18$ *for each* $i = 1, 2, 3$;
(2) *if* $\sec_i$ *is elliptic, then* $|\sec_i| \leqslant 15$;
(3) *if* $\sec_i$ *is elliptic and* $|\sec_i| > 13$, *then* $|\Gamma| \leqslant 52$. $\lhd$

Remark 3.10. In view of Lemma 3.9, the compatibility condition (3.5) simplifies to the form

$$\pi \vdash \theta_1 \quad \text{if} \quad 3|\theta_1| + |\pi| \geqslant 52 \text{ and } \theta_1 \preccurlyeq \pi$$

more consistent with (3.6) and (3.7). Indeed, if θ_1 is elliptic, we can assume that $|\theta_1| \leqslant 13$; then necessarily $|\pi| \geqslant 13$, see (3.5), and $\theta_1 \preccurlyeq \pi$ holds automatically.

Lemma 3.11. *If* $\Pi \subset \Gamma$ *is a maximal, with respect to* (3.2), *triangular pencil and* $|\Gamma| > 52$, *then* $|\Pi| \geqslant 14$.

Proof. As explained in Remark 3.10, in view of Lemma 3.9 we have $|\Pi| \geqslant 13$ and $|\sec_3| \leqslant |\sec_2| \leqslant |\sec_1| \leqslant |\Pi|$. If $|\Pi| = 13$, then $|\sec_3| = |\sec_2| = |\sec_1| = 13$ by (3.5) and, moreover, Π must have a multiple section s. Assuming that $s \cdot c_1 = s \cdot c_2 = 1$, so that c_1, c_2, s constitute a triangle, the union $(c_1, c_2, s) \sqcup \sec_3 \subset \Gamma$ is a triangular pencil (see Lemma 3.3) with 16 vertices, contradicting the maximality of Π. $\square$

3.2. Abundant collections.
Let $\Gamma_0 \supset \Sigma = (c_1, c_2, c_3) \cong \tilde{\mathbf{A}}_2$ be a triangular graph, $i = \varnothing, 1, 2, 3$ a parameter, and $\theta \in \mathcal{P}$ (if $i = \varnothing$) or $\theta \in \mathcal{T}$ (otherwise) a pattern. An overgraph $\Gamma \supset \Gamma_0$ is said to *represent* $(\Gamma_0, \theta)_i$ if

$$\sec(\Gamma \supset \Sigma \ni c_i) \in \theta \quad \text{and} \quad \Gamma \smallsetminus \sec_i = \Gamma_0, \quad \text{if } i = 1, 2, 3$$
$$\Pi(\Gamma \supset \Sigma) \in \theta \quad \text{and} \quad \Gamma \smallsetminus \Pi = \Gamma_0 \smallsetminus \Sigma, \quad \text{if } i = \varnothing.$$

A pair $(\Gamma_0, \theta)_i$ is called *abundant* if it cannot be represented by an acceptable graph, see Remark 2.10. Both notions extend to a collection $\mathcal{G}$ of graphs: Γ represents $(\mathcal{G}, \theta)_i$ if it represents $(\Gamma_0, \theta)_i$ for a graph $\Gamma_0 \in \mathcal{G}$, and $(\mathcal{G}, \theta)_i$ is abundant if so is each $(\Gamma_0, \theta)_i$, $\Gamma_0 \in \mathcal{G}$. Iterating, we extend both notions to a compatible (*i.e.*, satisfying the compatibility conditions from §3.1) collection of patterns

$$\pi \in \mathcal{P}, \quad \theta_i \in \mathcal{T}, \ i = 1, \dots, n \leqslant 3.$$

Clearly, if $\pi \vdash \dots \vdash \theta_n$ is abundant, so is any $\pi' \vdash \dots \vdash \theta_n'$ with $\pi \lhd \pi'$, $\dots$, $\theta_n \lhd \theta_n'$.

Our proof of Theorem 1.1 essentially reduces to applying the algorithm in §3.3 below to show that any compatible collection $\pi \vdash \theta_1 \vdash \theta_2 \vdash \theta_3$ is abundant: indeed, conditions (3.5)–(3.7) guarantee that on the way we will encounter *all* subgeometric graphs Γ such that either $|\Gamma| > 52$ or $\operatorname{rk} \Gamma = 20$, and in the latter case it would suffice to analyze all geometric saturations of Γ. To this end, we introduce the inductive notion of a *ruled out collection*:

- any abundant compatible collection is considered ruled out;
- in general, a compatible collection $\pi \vdash \theta_1 \vdash \dots \vdash \theta_n$, $n \leqslant 2$, is ruled out if so is *any* compatible extension $(\pi \vdash \theta_1 \vdash \dots \vdash \theta_n) \vdash \theta_{n+1}$, $\theta_{n+1} \in \mathcal{T}$.

By a machine aided computation, we establish the following statement; its proof is given in §3.6, after we collect all the necessary facts in §3.3, §3.4 and §3.5.

Proposition 3.12 (see §3.6). *Each compatible pair* $\pi \vdash \theta_1$, *where*

$$\pi \in \mathcal{P}_{14} := \{\pi \in \mathcal{P} \mid |\pi| \geqslant 14\} \quad \text{and} \quad \theta \in \mathcal{T},$$

is ruled out.

By the very definition, the assertion of Proposition 3.12 means that, for each representative Γ of any compatible collection $\pi \vdash \theta_1 \vdash \theta_2 \vdash \theta_3$, $\pi \in \mathcal{P}_{14}$, one has either $|\Gamma| = 52$ or $\operatorname{rk} \Gamma = 20$, and, moreover, all such representatives are encountered in the course of the proof. The latter fact enables us to obtain the complete list of representatives Γ of compatible collections $\pi \vdash \theta_1 \vdash \theta_2 \vdash \theta_3$, $\pi \in \mathcal{P}_{14}$, such that $|\Gamma| > 52$ and $\operatorname{rk} \Gamma = 20$ (see Addendum 3.23).

3.3. **Extending a graph by a triangular set.** The heart of the computation is an algorithm extending a given subgeometric graph Γ_0 by a given pattern $\theta \in \mathcal{T}$, the goal being listing all subgeometric overgraphs $\Gamma \supset \Gamma_0$ representing $(\Gamma_0, \theta)_i$ (where $i = \varnothing, 1, 2, 3$ is also fixed, see §3.2). The elements of $\Gamma \smallsetminus \Gamma_0$ are referred to as sections, whereas the connected components of $\Gamma \smallsetminus \Gamma_0 \in \theta$ are *polysections*. The algorithm is similar to that of [2], except that we can no longer guarantee that the sections are pairwise disjoint. Therefore, instead of adding to Γ one section at time, we fix θ in advance and add whole polysections, in the order $\tilde{\mathbf{A}}_2$, $\mathbf{A}_3$, $\mathbf{A}_2$, $\mathbf{A}_1$.

Convention 3.13. From now on, following [2, § A.3], we identify a section v with its *support*

$$\operatorname{supp} v := \big\{ u \in \Gamma_0 \mid v \cdot u = 1 \big\}$$

and thus treat it as a subset of Γ_0. We also keep the notation

$$\Gamma_0 \sqcup \mathbf{v} \quad \text{and} \quad \Gamma_0 \sqcup \mathbf{v}(\mathfrak{m})$$

for a multiset $\mathbf{v}$ (which we no longer assume sorted) and $(|\mathbf{v}| \times |\mathbf{v}|)$-matrix $\mathfrak{m}$. As explained in §2.3, only acceptable graphs are retained after each step.

In practice, we start with computing the group $G_0 := \operatorname{Aut} \Gamma_0$ and set

$$(3.14) \qquad \mathcal{S}(\Gamma_0) := \big\{ s \subset \Gamma_0 \mid s \cap \Sigma = \underline{\text{fixed}} \big\}$$

of sections of Γ_0 satisfying extra conditions imposed by the problem at hand. (Here, $\underline{\text{fixed}} \subset \Sigma$ is a certain subset fixed in advance. We can also take into account a few obvious geometric restrictions, but this is not crucial: "wrong" sections are immediately ruled out by the preliminary tests in §2.3(1). We omit many other technical tweaks, referring to the code [4] as the ultimate source.) Then, running the tests cited in §2.3(2) and (3), we compute the sets

$$(3.15) \qquad \begin{aligned} \mathbf{A}_1(\Gamma_0) &:= \big\{ v \in \mathcal{S}(\Gamma_0) \mid \Gamma_0 \sqcup v \text{ is acceptable} \big\}, \\ \mathfrak{m}(\Gamma_0) &:= \big\{ \mathbf{v} \in \mathbf{A}_1(\Gamma_0)^{\dim \mathfrak{m}} \mid \Gamma_0 \sqcup \mathbf{v}(\mathfrak{m}) \text{ is acceptable} \big\}, \end{aligned}$$

where $\mathfrak{m} = \mathbf{A}_2$, $\tilde{\mathbf{A}}_2$, $2\mathbf{A}_1$, $\mathbf{A}_3$ (in this order). Certainly, the tests are applied to a single representative of each G_0-orbit; in what follows (*cf.*, *e.g.*, Remark 3.19) this convention is taken for granted. This computation is aborted if a "required" list is empty (*e.g.*, if $\mathbf{A}_2(\Gamma_0) = \varnothing$ whereas θ contains $\tilde{\mathbf{A}}_2$ or $\mathbf{A}_3$, *cf.* the next remark).

Remark 3.16 (a technical detail). The set $\mathbf{A}_2(\Gamma_0)$ is used in the computation of $\tilde{\mathbf{A}}_2(\Gamma_0)$: we consider only those triples (v_1, v_2, v_3) for which $(v_i, v_j) \in \mathbf{A}_2(\Gamma_0)$ for all $1 \leqslant i < j \leqslant 3$. Likewise, both $\mathbf{A}_2(\Gamma_0)$ and $2\mathbf{A}_1(\Gamma_0)$ are used in the computation of $\mathbf{A}_3(\Gamma_0)$. Furthermore, $2\mathbf{A}_1(\Gamma_0)$ is used at all subsequent steps: when iterating

$$\Gamma_{n-1} \sqcup \mathbf{v}(\mathfrak{m}_n) = \big(\Gamma_0 \sqcup \mathbf{u}(\cdot) \big) \sqcup \mathbf{v}(\mathfrak{m}_n),$$

in (3.17) below, we check first that $(u, v) \in 2\mathbf{A}_1(\Gamma_0)$ for all $u \in \mathbf{u}$, $v \in \mathbf{v}$.

Now, let $\theta = \tilde{a}_2\tilde{\mathbf{A}}_2 + a_3\mathbf{A}_3 + a_2\mathbf{A}_2 + a_1\mathbf{A}_1$, so that $N := \tilde{a}_2 + a_3 + a_2 + a_1$ is the number of components, and let $\mathfrak{m}_1 \geqslant \ldots \geqslant \mathfrak{m}_N$ be the types of the components of θ ordered via $\tilde{\mathbf{A}}_2 > \mathbf{A}_3 > \mathbf{A}_2 > \mathbf{A}_1$). Then, we start from

$$\mathfrak{S}_0 := \{\Gamma_0\}$$

and run the computation in up to N steps.

Step $n \geqslant 1$: for each graph $\Gamma_{n-1} \in \mathfrak{S}_{n-1}$, we pick a single representative $\mathbf{v}$ of each $(\mathrm{Aut}\,\Gamma_{n-1})$-orbit on $\mathfrak{m}_n(\Gamma_0)$ and use the tests of §2.3(2) and (3) to compute

$$(3.17) \qquad \mathfrak{S}_n(\Gamma_{n-1}) := \big\{\Gamma_{\mathbf{v}} := \Gamma_{n-1} \sqcup \mathbf{v}(\mathfrak{m}_n) \,\big|\, \Gamma_{\mathbf{v}} \text{ is acceptable}\big\}.$$

The step concludes by uniting all sets $\mathfrak{S}_n(\Gamma_{n-1})$, $\Gamma_{n-1} \in \mathfrak{S}_{n-1}$, obtained followed by retaining a single representative of each graph isomorphism class.

The algorithm terminates either upon the completion of Step N (resulting in a list $\mathfrak{S}_N(\Gamma_0)$ to be processed by other means) or when one of the previous steps results in an empty list $\mathfrak{S}_n(\Gamma_0) = \varnothing$, implying that (Γ_0, θ) is abundant.

Remark 3.18. Both auto- and isomorphisms of graphs are computed using the `digraph` package in `GAP` [9]. All morphisms are restricted: we assume the fiber Σ fixed as a set and, typically, one or two edges $c_i \in \Sigma$ fixed pointwise, so that the set $\mathcal{S}(\Gamma_0)$ in (3.14) be invariant.

Remark 3.19 (a technical detail). Each time the matrix $\mathfrak{m}$ changes, *i.e.*, whenever $\mathfrak{m}_n > \mathfrak{m}_{n+1}$, we recompute the (relevant) sets $\mathfrak{m}(\Gamma_n)$ for each graph $\Gamma_n \in \mathfrak{S}_n$ and use these new lists in the subsequent steps. Instead of starting from scratch, as in the case of Γ_0, we merely run the tests on the ready lists $\mathfrak{m}(\Gamma_m)$ for the last subgraph $\Gamma_m \subset \Gamma_n$ for which they have been computed.

3.4. **Processing several patterns.** The material of this section is of a purely technical nature; however, it is the tweak described here that makes the computation much faster and eventually helps it to terminate reasonably fast.

Typically, we fix a subgeometric graph Γ_0 and try to rule out a whole collection of patterns $\mathcal{T}(\Gamma_0)$. Since patterns tend to have similar initial sequences, processing them all one-by-one would force us to repeat the same steps of the computation over and over again. To avoid the repetition and remove a number of redundant steps, we sort the patterns in the *direct* lexicographic order and process them simultaneously, organizing the computation into four layers: the outermost $\tilde{\mathbf{A}}_2$, $\mathbf{A}_3$, $\mathbf{A}_2$, and the innermost $\mathbf{A}_1$.

Each inner layer starts from a certain intermediate graph Γ and processes a collection of patterns $\mathcal{T}(\Gamma)$. If the algorithm terminates prematurely, at a certain pattern θ, we conclude that (Γ, θ) is abundant, and hence so is (Γ, θ') whenever $\theta \lhd \theta'$. This fact is reported to the previous layer, where the information is consolidated and often results in excluding the graph Γ and/or some patterns from the further consideration. We refer to the code [4] for the precise details (we implement each next layer as a hook within the previous one, where it is used to modify the intermediate lists); here, we merely illustrate the paradigm by the following simple example.

Example 3.20. Assume that the patterns to be considered are

$$\mathcal{T}(\Gamma_0) = \big\{2\mathbf{A}_2 \oplus 6\mathbf{A}_1, 3\mathbf{A}_2 \oplus 4\mathbf{A}_1, 4\mathbf{A}_2 \oplus 2\mathbf{A}_1\big\},$$

so that only two layers of computation are required. We run the first two steps of the $\mathbf{A}_2$-layer, resulting, say, in a list $\mathfrak{S}_2 = \{\Gamma'_2, \Gamma''_2\}$, and switch to the $\mathbf{A}_1$-layer for each of the two graphs. Assume that this inner layer terminates at

- step 4 for $\Gamma'_2 \Rightarrow (\Gamma'_2, 4\mathbf{A}_1)$, $(\Gamma'_2, \mathbf{A}_2 \oplus 3\mathbf{A}_1)$, $(\Gamma'_2, 2\mathbf{A}_2 \oplus 2\mathbf{A}_1)$ are abundant,
- step 5 for $\Gamma''_2 \Rightarrow (\Gamma''_2, 5\mathbf{A}_1)$, $(\Gamma''_2, \mathbf{A}_2 \oplus 4\mathbf{A}_1)$ are abundant.

(Obviously, $4\mathbf{A}_1 \lhd \mathbf{A}_2 \oplus 3\mathbf{A}_1 \lhd 2\mathbf{A}_2 \oplus 2\mathbf{A}_1$ and $5\mathbf{A}_1 \lhd \mathbf{A}_2 \oplus 4\mathbf{A}_1$.) We conclude that Γ'_2 can be excluded from $\mathfrak{S}_2$ and that both $2\mathbf{A}_2 \oplus 6\mathbf{A}_1$ and $3\mathbf{A}_2 \oplus 4\mathbf{A}_1$ can be excluded from $\mathcal{T}(\Gamma_0)$. Therefore, we can run *two* more steps of the $\mathbf{A}_2$-layer on the new reduced list $\{\Gamma''_2\}$, followed by the $\mathbf{A}_1$-layer on the result. (The $\mathbf{A}_1$-layer after Step 3 can be skipped as $\theta = 3\mathbf{A}_2 \oplus 4\mathbf{A}_1$ has already been ruled out!)

If it were not for Γ''_2 (*e.g.*, if the $\mathbf{A}_1$-layer terminated at a step $\leqslant 4$ for each of the two graphs), we would have stopped immediately, as all elements of $\mathcal{T}(\Gamma_0)$ would have been ruled out by the $\mathbf{A}_1$-layer after Step 2.

3.5. **The aggressive version.** In certain cases, one can argue that, in order to achieve the goal $|\Gamma| \geqslant 53$, the overgraph $\Gamma \supset \Gamma_0$ must be spanned over Γ_0 by a few pairwise disjoint vertices *independent* over Γ_0. (Precisely, this condition means that $\mathcal{F}(\Gamma) \otimes \mathbb{Q}$ is generated over $\mathcal{F}(\Gamma_0) \otimes \mathbb{Q}$ by $(\mathrm{rk}\,\Gamma - \mathrm{rk}\,\Gamma_0)$ pairwise disjoint vertices.) In this case, we switch to the *aggressive version* of the algorithm, *i.e.*, we

- add disjoint vertices only (the $\mathbf{A}_1$-layer),
- disregard the extra vertices that do not increase rank, and
- check the saturation lists of all intermediate graphs, including Γ_0,

cf. the *progressive mode* in [2, § A.4.4].

Precisely, this approach is used

- in the proof of Lemma 3.9(3): we add up to two disjoint vertices, and
- at the steps $\underline{\text{fixed}} = \{c_2\}$ or $\{c_3\}$ in §3.6 below (*cf.* also Remark 4.11), when extending a graph Γ_0 of the submaximal rank $\mathrm{rk}\,\Gamma_0 = 19$.

3.6. **Proof of Proposition 3.12.** As stated, the proof is an explicit machine aided computation using the algorithm described in §3.3 and §3.4. It runs in two steps: first, for each pattern $\theta_1 \in \mathcal{T}$, we rule out *almost* all compatible patterns $\pi \in \mathcal{P}_{14}$; the set of these patterns is denoted by $\mathcal{P}_{14}^-(\theta_1)$. Then, for each $\pi \in \mathcal{P}_{14}$, we rule out the remaining patterns $\theta_1 \in \mathcal{T}$ such that $\pi \vdash \theta_1$ and $\pi \notin \mathcal{P}_{14}^-(\theta_1)$.

Remark 3.21. The choice of the set $\mathcal{P}_{14}^-(\theta_1)$ at the first step looks quite arbitrary, and indeed so it is. *As a rule*, we let $\pi \in \mathcal{P}_{14}^-(\theta_1)$ if $\pi \vdash \theta_1$ and

$$\mathrm{rk}\,\pi \leqslant \mathrm{rk}(\Sigma \sqcup_1 \theta_1).$$

However, a few border cases are subject to further manual tweaking, which is based on experiments. More precisely, depending on the values $r := \mathrm{rk}(\Sigma \sqcup_1 \theta_1)$, $n := |\theta_1|$, the following coefficient quadruples $(\tilde{a}_2, a_3, a_2, a_1)$ are *excluded* from $\mathcal{P}_{14}^-(\theta_1)$:

$$
\begin{aligned}
(r, n) = (12, 11): \quad & (*, *, *, *), \\
(12, 12): \quad & (*, *, *, *), \\
(13, 11): \quad & (*, *, *, *), \\
(13, 12): \quad & (3, *, *, *), (2, *, *, *), (1, *, *, *), \\
(13, 13): \quad & (2, *, *, *), (1, *, *, *), \\
(14, 11): \quad & (*, *, *, *),
\end{aligned}
$$

$$
\begin{aligned}
(14, 12)\colon \quad & (3, *, *, *), (2, *, *, *), (1, *, *, *), \\
(14, 13)\colon \quad & (2, *, *, *), (1, *, *, *), \\
(14, 14)\colon \quad & (2, *, *, *), (1, *, *, *), \\
(15, 11)\colon \quad & (*, *, *, *), \\
(15, 13)\colon \quad & (2, 0, 0, *), (1, 0, *, *), \\
(15, 14)\colon \quad & (2, 1, 0, *), (2, 0, *, *), (1, 0, *, *), \\
(15, 15)\colon \quad & (1, *, *, *)
\end{aligned}
$$

(where, as usual, $*$ means any value).

At the first step, we start with the graph

$$
\Gamma_0 := \Sigma \sqcup_1 \Theta_1, \quad \Theta_1 \in \theta_1 \in \mathcal{T},
$$

and use §3.4 to find all graphs Γ representing $(\Gamma_0, \pi)_\varnothing$, $\pi \in \mathcal{P}_{14}^-(\theta_1)$. Technically, we extend Γ_0 by a pattern θ such that $\tilde{\mathbf{A}}_2 \oplus \theta = \pi$. Thus, we let $\underline{\text{fixed}} = \varnothing$ in (3.14) and use graph auto-/isomorphisms preserving $\Sigma \ni c_1$ (see Remark 3.18). For each graph Γ on the resulting list $\mathfrak{S}_N$, we consider the full set $\mathcal{T}(\Gamma)$ of patterns $\theta_2 \in \mathcal{T}$ satisfying (3.6), and run the same algorithm with $\underline{\text{fixed}} = \{c_2\}$ and graph morphisms preserving c_1 and c_2.

Remark 3.22. Strictly speaking, we should have run the algorithm once more, using $\underline{\text{fixed}} = \{c_3\}$ and patterns θ_3 satisfying (3.7). However, our thresholds are chosen so that the list $\mathfrak{S}_N$ resulting from the first run consists of relatively few graphs of rank 19 (for which the aggressive version is used, see §3.5) and very few graphs of rank 18, for which the algorithm terminates fast and rules everything out.

At the second step, we start with a pencil

$$
\Gamma_0 := \Pi \in \pi \in \mathcal{P}_{14}
$$

and use §3.4 to find all graphs Γ representing $(\Gamma_0, \theta_1)_1$, $\pi \vdash \theta_1$ and $\pi \notin \mathcal{P}_{14}^-(\theta_1)$. We let $\underline{\text{fixed}} = \{c_1\}$ in (3.14) and use graph morphisms preserving $\Sigma \ni c_1$. As above, the relatively few graphs obtained, all of rank 19 or 18, are ruled out by the next run, using $\underline{\text{fixed}} = \{c_2\}$ and $\theta_2 \in \mathcal{T}$ compatible in the sense of (3.6). This completes the proof of Proposition 3.12, as well as of Addendum 3.23 below. □

As explained right after Proposition 3.12, before discarding a graph Γ of rank 20, we analyze its geometric finite index extensions and record those of size greater than 52. The result of this analysis is stated below.

Addendum 3.23. *Let Γ be a geometric representative of a compatible collection $\pi \vdash \theta_1 \vdash \theta_2 \vdash \theta_3$, $\pi \in \mathcal{P}_{14}$, such that $\operatorname{rk}\Gamma = 20$ and $|\Gamma| > 52$. Then Γ is one of the eight smooth configurations found in [8], see the first eight rows of Table 1.* ◁

Remark 3.24. In order to produce a plethora of examples of large configurations of lines, when discarding the graphs of rank 20 (see Remark 2.10) we collected all extended graphs with at least 48 lines or at least six exceptional divisors; the results are found in [4]. In particular, in addition to the surfaces listed in Table 1, we found but one quartic with 52 lines and two nodes and two quartics with 50 lines and one node each. Besides, there are quite a few quartics with non-empty singular locus and 48 lines, suggesting once again that 48 is a reasonable threshold to cut the classification.

4. Smooth quartics

In this section we temporarily assume that the polarized lattice $S \ni h$ contains no exceptional divisors; this will be used later in our study of line configurations on smooth quartic surfaces $X_4 \subset \mathbb{P}^3$.

In this case, we need to change the notion of admissible lattice/graph. Namely, a polarized lattice $S \ni h$ is called *smooth*, or *s-admissible*, if it contains neither exceptional divisors ($e^2 = -2$, $e \cdot h = 0$) nor 2-isotropic vectors ($e^2 = 0$, $e \cdot h = 2$). A graph Γ is *smooth*, or *s-admissible*, if so is the lattice $\mathcal{F}(\Gamma)$.

If $S \ni h$ is smooth, then $\mathfrak{rt}(S, h) = \varnothing$; hence, automatically, $\Delta = \varnothing$ in (2.2) and we have a well-defined Fano graph

$$(4.1) \qquad \operatorname{Fn}(S, h) := \operatorname{Fn}_\varnothing(S, h) = \operatorname{root}_1(S, h).$$

An crucial consequence of (4.1) is the fact that Fn is monotonous:

$$(4.2) \qquad \text{if } S' \supset S \ni h \text{ are smooth, then } \operatorname{Fn}(S', h) \supset \operatorname{Fn}(S, h).$$

Lemma 4.3. *Let Γ be a smooth graph and $\Sigma = (c_1, c_2, c_3) \subset \Gamma$ a triangle. Then*:
  (1) *Σ has a unique 3-section $c_0 := h - c_1 - c_2 - c_3 \in \Gamma$;*
  (2) *the pencil Π as in (2.11) and $\triangle$-sets $\sec_i$ as in (2.13) have no connected components of types $\mathbf{A}_2$ or $\mathbf{A}_3$.*

Proof. Clearly, c_0 as in Statement (1) is a 3-section in the lattice spanned by h and Σ. By (4.2), it remains a 3-section in any larger *smooth* lattice/graph.

If the pencil Π has a pair $(s_1, s_2) \cong \mathbf{A}_2$, by (4.2) it also has $s_3 := \kappa_\Sigma - s_1 - s_2$, so that $(s_1, s_2, s_3) \cong \tilde{\mathbf{A}}_2$. If Π has $(s_1, s_2, s_3) \cong \mathbf{A}_3$, then $\kappa_\Sigma - s_1 - s_2 - s_3$ is an exceptional divisor. The same argument applies to each set $\sec_i$, $i = 1, 2, 3$, except that we replace κ_Σ with $(c_0 + \ldots + c_3) - c_i = \kappa_\Sigma + c_0 - c_i$. $\square$

In view of Lemma 4.3(1), each type $\tilde{\mathbf{A}}_2$ fiber $\Sigma_0 := \Sigma = (c_1, c_2, c_3)$ gives rise to three more, *viz.* $\Sigma_i := (c_0, \ldots, \hat{c}_i, \ldots)$, $i = 1, 2, 3$ (where, as usual, $\hat{c}_i$ indicates that c_i has been omitted). Thus, we can shift the paradigm and, instead of considering a pencil Π and three sets $\sec_i$, we can speak about "blending" four pencils

$$\Pi_0 := \Pi = \Pi(\Gamma \supset \Sigma_0), \qquad \Pi_i := \Sigma_i \sqcup \sec_i = \Pi(\Gamma \supset \Sigma_i), \quad i = 1, 2, 3.$$

Assuming, as above, that Π is a maximal pencil in Γ, we can replace (3.5)–(3.7) with a stronger set of compatibility conditions:

$$(4.4) \qquad \pi \vdash \theta_1 \quad \text{if} \quad 3|\theta_1| + |\pi| \geqslant 48 \text{ and } \theta_1' \preccurlyeq \pi;$$

$$(4.5) \qquad (\pi \vdash \theta_1) \vdash \theta_2 \quad \text{if} \quad 2|\theta_2| + |\theta_1| + |\pi| \geqslant 48 \text{ and } \theta_2' \preccurlyeq \theta_1';$$

$$(4.6) \qquad (\pi \vdash \theta_1 \vdash \theta_2) \vdash \theta_3 \quad \text{if} \quad |\theta_3| + |\theta_2| + |\theta_1| + |\pi| \geqslant 48 \text{ and } \theta_3' \preccurlyeq \theta_2'.$$

Here, $'$ stands for the operator $\Theta \mapsto \Theta' := \tilde{\mathbf{A}}_2 \sqcup \Theta$ and its natural descent to the set of patterns. (Recall also that, for Theorem 1.2, we need to change the threshold to $|\Gamma| \geqslant 49$.) In particular, from (4.4)–(4.6) we immediately conclude that

$$(4.7) \qquad |\Pi| \geqslant 15,$$

cf. Lemma 3.11. Indeed, taking into account the 3-section given by Lemma 4.3, we can rewrite (4.6) in the form $|\theta_3'| + |\theta_2'| + |\theta_1'| + |\pi| \geqslant 57 = 48 + 9$, and it remains to observe that the assumption $\theta_3' \preccurlyeq \theta_2' \preccurlyeq \theta_1' \preccurlyeq \pi$ implies $|\theta_3'| \leqslant |\theta_2'| \leqslant |\theta_1'| \leqslant |\pi|$. Thus, unlike Proposition 3.12, we do not need to introduce an analogue $\mathcal{P}_{15}^s$ of the set $\mathcal{P}_{14}$: the lower bound (4.7) would follow from the compatibility assumptions.

Now, a computation similar to (but much faster than) that of §3 yields the following result (*cf.* Proposition 3.12; we retain the terminology of §3 and denote by $\mathcal{P}^{\mathrm{s}} \subset \mathcal{P}$ and $\mathcal{T}^{\mathrm{s}} \subset \mathcal{T}$ the sets of patterns appearing in smooth graphs).

Proposition 4.8 (*cf.* §3.6). *Each compatible collection* $\pi \vdash \theta_1 \vdash \theta_2 \vdash \theta_3$, *as in* (4.4)–(4.6), *with* $\pi \in \mathcal{P}^{\mathrm{s}}$ *and* $\theta_1, \theta_2, \theta_3 \in \mathcal{T}^{\mathrm{s}}$, *either is ruled out or has one of the five graphs*

$$(4.9) \qquad\qquad \mathbf{Z}_{49}, \quad (50), \quad \mathbf{Z}_{50}, \quad (52), \quad \mathbf{Z}_{52}$$

(*see* Table 1) *as a geometric representative.*   ◁

Similar to Proposition 3.12, this statement means that, with the five exceptions listed in (4.9), any geometric representative Γ of a collection as in the hypotheses has $\mathrm{rk}\,\Gamma = 20$ and, moreover, all such representatives of rank 20 are encountered and discarded in the course of the proof. As in §3, prior to discarding a graph we compute all its geometric finite index extensions, thus arriving at the following complete list of geometric rank 20 Fano graphs Γ with $|\Gamma| \geqslant 48 + 1$ (the extra 1 standing for the 3-section given by Lemma 4.3).

Addendum 4.10. *Let* Γ *be a geometric representative of a compatible collection* $\pi \vdash \theta_1 \vdash \theta_2 \vdash \theta_3$ *as in* (4.4)–(4.6), *where* $\pi \in \mathcal{P}^{\mathrm{s}}$, $\theta_1, \theta_2, \theta_3 \in \mathcal{T}^{\mathrm{s}}$, *and* $\mathrm{rk}\,\Gamma = 20$. *Then* Γ *is one of the* 21 *smooth rank* 20 *configurations found in* Table 1.   ◁

Remark 4.11. Due to the lower threshold $|\Gamma| \geqslant 49$, occasionally we do have to run the algorithm till the very last step $\underline{\mathrm{fixed}} = \{c_3\}$, *cf.* Remark 3.22. This last step is quite expensive (as the set of sections to begin with is quite large), but fortunately it has to be done for four graphs only. This is yet another indication of the fact that taking the classification down to 48 or fewer lines is hardly feasible.

Remark 4.12. In the smooth case, we can further reduce the overcounting by a number of tricks based on the monotonicity property (4.2), using all lines present in the lattice rather than only those added explicitly. Most notably, before switching to a next step $\underline{\mathrm{fixed}} = \{c_i\}$, $i \leqslant 3$, we can replace each graph Γ with the union

$$\Pi \cup \mathrm{sec}_1 \cup \ldots \cup \mathrm{sec}_{i-1} \quad \text{in} \quad \mathrm{Fn}(\mathcal{F}(\Gamma))$$

and then retain a single representative of each isomorphism class of the list obtained. Furthermore, in the subsequent computation we can impose an extra condition that the above union should remain fixed. We refer to [5] for further details.

5. Quadrangular graphs

In this section the $K3$-quartic X_4 is allowed to have singular points as in §3. Consider an $\tilde{\mathbf{A}}_3$-graph Γ and fix a quadrangle $\Sigma := (c_1, c_2, c_3, c_4) \subset \Gamma$. We assume the edges $c_i \in \Sigma$ numbered cyclically and ordered consecutively:

$$c_{i+4} = c_i, \qquad c_i \cdot c_{i\pm 1} = 1, \quad c_i \cdot c_{i\pm 2} = 0.$$

In addition to (2.11)–(2.13), we consider the sets

$$\mathrm{sec}^*_{ij} := \mathrm{sec}^*_i \cup \mathrm{sec}^*_j, \quad i = j \pm 2.$$

The assumption that $\mathrm{girth}(\Gamma) = 4$ implies that

$$\mathrm{sec}^*_{13} \cap \mathrm{sec}^*_{24} = \varnothing \qquad \text{and} \qquad \text{each graph } \mathrm{sec}^*_i \text{ is discrete.}$$

The elements of each $\sec_i$ are simple sections of Π, and those of

$$\sec_i^* \smallsetminus \sec_i = \sec_j^* \smallsetminus \sec_j = \sec_i^* \cap \sec_j^*, \quad j = i \pm 2,$$

are double sections; the set of all (multi-)sections of Π is $\sec^* = \sec_{13}^* \cup \sec_{24}^*$.

From now on, we state our results for *geometric* rather than subgeometric graphs; in other words, we assume that Γ admits a *triangle free* geometric saturation.

Lemma 5.1. *In a geometric quadrangular graph $\Gamma \supset \Sigma$ as above, one has*

(1) $|\sec_i| \leqslant 10$ *and* $|\sec_i^*| \leqslant 10$ *(sharp bounds),*
(2) $|\sec_{ij}^*| \leqslant 20$ *(a sharp bound), and*
(3) $|\sec^*| \leqslant 32$ *(the best known example being 30).*

Proof. Statement (1) is a direct computation: since each $\sec_i^*$ is discrete, the union $\Sigma \cup \sec_i^*$ depends on just two parameters, which can take the following values:

$$(5.2) \qquad \begin{array}{llllllllllll} p_i := |\sec_i| & = & 0 & 1 & 2 & 3 & 4 & 5 & 6 & 7 & 8 & 9 & 10 \\ q_i := |\sec_i^* \smallsetminus \Theta_i| & \leqslant & 8 & 7 & 6 & 5 & 5 & 4 & 4 & 3 & 2 & 1 & 0 \end{array}$$

The bound in (2) follows from (1) (assuming $p_i \geqslant p_j$, we have $|\sec_{ij}^*| \leqslant 2p_i + q_i$), and its sharpness is established by an explicit construction (obtained in the next computation). Finally, statement (3) is also obtained by a computation similar to [2, §B.5]: assuming that

$$(5.3) \qquad |\sec_1| \geqslant |\sec_3|, \quad |\sec_2| \geqslant |\sec_4|, \quad |\sec_{13}^*| \geqslant |\sec_{24}^*|,$$

we start with a "standard" graph $\Sigma \cup \sec_1^*$, letting $(p_1, q_1) = (10, 0)$, $(9, 1)$, $(9, 0)$, $(8, 2)$, $(8, 1)$, or $(7, 3)$, and build all possible consecutive extensions

$$(5.4) \qquad \Gamma := (\Sigma \cup \sec_1^*) \cup \sec_3 \cup \sec_2 \cup (\sec_2^* \smallsetminus \sec_2) \cup \sec_4$$

via discrete sets; the minimal size of each set to be added is determined using (5.2), (5.3), and the goal $|\Gamma| \geqslant 37$. In most cases, this algorithm terminates (meaning that each sufficiently large graph admitting a geometric *triangle free* saturation is unacceptable, *cf.* Remark 2.10) at the very first nontrivial step $\sec_3$; in very few cases we also need to use $\sec_2$. $\qquad\square$

Remark 5.5. In the proof of Lemma 5.1 and Proposition 5.6 below, the essential difference from [2] is that we do not limit the number of lines intersecting both given ones (the presence of biquadrangles and longer "polyquadrangles"); this makes the computation slightly more involved.

Proposition 5.6. *For a geometric quadrangular graph Γ one has $|\Gamma| \leqslant 48$.*

Remark 5.7. It is unlikely that the bound given by Proposition 5.6 is sharp: the best example that we found has 39 lines (see also [2, Proposition 6.14]).

Proof of Proposition 5.6. The proof is a computation similar to [2, §C.3]. In view of Lemma 5.1, it suffices to consider all quadrangular pencils Π of size $|\Pi| \geqslant 17$; the list of such pencils admitting a polarization is compiled using [21]. Then, under the assumptions of (5.3), we must have $4p_1 + 2q_1 + |\Pi| \geqslant 49$. Similar to (5.4), we start from a pencil Π and build a list of consecutive acceptable extensions

$$\Gamma := \Pi \cup \sec_1 \cup (\sec_1^* \smallsetminus \sec_1) \cup \sec_3 \cup \sec_2 \cup (\sec_2^* \smallsetminus \sec_2) \cup \sec_4.$$

Due to our modest goal $|\Gamma| \geqslant 49$, *de facto* the algorithm terminates at the first or, occasionally, second step, so that we never need to consider even $\sec_3$. $\qquad\square$

6. Other types of graphs

For the other types (in the sense of §2.4) of graph, the computation runs exactly as in [2], and we merely state the updated results below. Remarkably, the upper bounds obtained are exactly the same as in the smooth case (see [5]); furthermore, unlike the case of octics (see [2]), all extremal configurations are smooth.

6.1. **Pentagonal graphs.** Recall that the assumption girth$(\Gamma) = 5$ implies that, for a fiber $\tilde{\mathbf{A}}_4 \cong \Sigma \subset \Gamma$, one has

- $\sec^* = \sec_1 \cup \ldots \cup \sec_5$, *i.e.*, all sections are simple;
- each graph $\sec_i^* = \sec_i$, $i = 1, \ldots, 5$, is discrete.

The following bounds are sharp, and there are but two geometric pentagonal graphs with 30 vertices, *viz.* Φ'_{30} and Φ''_{30} (see [5]). Both represent configurations of lines on *smooth* quartic surfaces only.

Lemma 6.1 (*cf.* [2, Lemma 7.6]). *Let Γ be a geometric pentagonal graph, and let $\Sigma \subset \Gamma$ be a type $\tilde{\mathbf{A}}_4$ subgraph. Then*:

(1) *one has $|\sec_*| \leqslant 16$;*
(2) *if $|\sec_*| \geqslant 14$, then $|\Gamma| \leqslant 29$.*   ◁

Proposition 6.2. *One has $|\Gamma| \leqslant 30$ for any geometric pentagonal graph Π.*

Proof. In view of Lemma 6.1, it suffices to consider pentagonal pencils Π such that $|\Gamma| \geqslant 17$; they can be found using [21]. $\square$

6.2. **Astral graphs.** We number the vertices $(c_1, \ldots, c_5)$ of a type $\mathbf{D}_4$ fiber Σ so that the *central vertex* c_1 is the one of valency 4 in Σ. Recall that the assumption girth$(\Gamma) \geqslant 6$ implies that, for a fiber $\tilde{\mathbf{D}}_4 \cong \Sigma \subset \Gamma$ one has

- $\sec^* = \sec_1 \cup \ldots \cup \sec_5$, and
- the graph $\sec^*$ is discrete.

Note though that it is *not* true that all sections are simple: the elements of $\sec_1$ are double sections. (Recall that $\kappa_\Sigma = 2c_1 + c_2 + \ldots + c_5$.)

The following bounds are sharp, and the only geometric astral graph with 27 vertices is Δ'_{27} (see [5]); it is represented by a unique *smooth* quartic surface.

Lemma 6.3 (*cf.* [2, Lemma 7.3]). *Let Γ be a geometric astral graph and $\Sigma \subset \Gamma$ a type $\tilde{\mathbf{D}}_4$ subgraph whose central vertex c_1 has maximal valency in Γ. Then*:

(1) *one has $|\sec^*| \leqslant 12$;*
(2) *if $|\sec^*| \geqslant 11$, then $|\Gamma| \leqslant 27$.*   ◁

Proposition 6.4. *One has $|\Gamma| \leqslant 27$ for any geometric astral graph Π.*

Proof. In view of Lemma 6.3, it suffices to consider astral pencils Π with $|\Gamma| \geqslant 18$; they can be found using [21]. $\square$

6.3. **Locally elliptic graphs.** Let us recall, that the case of locally elliptic graphs was considered in [2]. We have the inequality

$$(6.5) \qquad\qquad\qquad |\Gamma| \leqslant 29$$

for all geometric locally elliptic graphs Γ (see [2, (7.1)]). Machine-aided experiments suggest that the sharp bound is $|\Gamma| \leqslant 25$ with a unique graph Λ_{25} that attains the maximum , but such considerations are of no importance for the proof of Theorem 1.1.

7. Proofs

In order to render our exposition self-contained, we recall certain results from [2] in §7.1, before presenting the proofs of the main results of the paper in §7.2, §7.3.

7.1. **Fano graphs of $K3$-quartics.** Let $X_4 \subset \mathbb{P}^3$ be a complex degree-4 surface with at worst Du Val (*aka* **A**–**D**–**E**, or simple) singularities and let $\pi\colon \tilde{X}_4 \to X_4$ be the minimal resolution of its singularities. Denote $h := \pi^* \mathcal{O}_{X_4}(1) \in \mathrm{NS}(\tilde{X}_4)$.

Recall that $\tilde{X}_4$ is a $K3$-surface. In particular, given an irreducible curve $C \subset \tilde{X}_4$, we have

(7.1) $C \cdot h = 1$ and $C^2 = -2$ if and only if $\pi(C)$ is a degree one curve on X_4.

The curves that satisfy (7.1) are called *lines* on $\tilde{X}_4$; they are obviously smooth and rational. We follow [5] and define the (*plain*) *Fano graph* of the quartic X_4 as the loop free graph with vertices

(7.2) $$\mathrm{Fn}(X_4) := \left\{ (-2)\text{-curves } C \subset \tilde{X}_4 \text{ with } C \cdot h = 1 \right\}$$

and each pair of vertices $v, w \in \mathrm{Fn}(X_4)$ connected by an edge of multiplicity $v \cdot w$. (Here and below, we always consider the intersection form "·" on $\mathrm{NS}(\tilde{X}_4)$.)

Recall that, by [2, (4.5)],

(7.3)   the graph $\mathrm{Fn}(X_4)$ of a $K3$-quartic with at least 25 lines is hyperbolic.

General theory of lattice-polarized $K3$-surfaces (Nikulin [15], Saint-Donat [19]; *cf.* also [8, Theorem 3.11] and [6, Theorem 7.3]) yields the following statement. (As in [2, Convention 1.4], we say that the lattice $\mathrm{NS}(\tilde{X}_4)$ is *spanned by lines* if it is a finite index extension of its sublattice generated by the classes of lines on $\tilde{X}_4$ *and the quasi-polarization h*, *i.e.*, it is spanned by lines and h over $\mathbb{Q}$.)

Theorem 7.4 (see [2, Theorem 3.9]). *A graph Γ is geometric if and only if one has $\Gamma \cong \mathrm{Fn}(X_4)$ for a quartic X_4 such that $\mathrm{NS}(\tilde{X}_4)$ is spanned by lines.*   ◁

Remark 7.5. As in the case of $K3$-octics, by [2, Lemma 2.8], in order to study the *maximal number of lines* we can restrict our attention to the case when the lattice $\mathrm{NS}(\tilde{X}_4)$ is spanned by lines and exceptional divisors (see also [2, § 8])

Obviously, for a quartic X_4 with non-empty singular locus the graph $\mathrm{Fn}(X_4)$ does not completely describe the configuration of lines on X_4. The latter can be inferred from the bi-colored *extended Fano graph*

(7.6) $$\mathrm{Fn}^{\mathrm{ex}}(X_4) := \left\{ (-2)\text{-curves } C \subset \tilde{X}_4 \text{ with } C \cdot h \leqslant 1 \right\},$$

with the colour of each vertex C defined as $C \cdot h$. For such graphs we have a more general statement.

Theorem 7.7 (see [2, Theorem 3.10]). *A bi-colored graph Γ' is geometric if and only if $\Gamma' \cong \mathrm{Fn}^{\mathrm{ex}}(X_4)$ for a $K3$-quartic $X_4 \subset \mathbb{P}^3$.*   ◁

7.2. **Proof of Theorem 1.1.** By Theorem 7.7, the assertion of Theorem 1.1 is equivalent to the statement that there are no

(7.8)   geometric bi-colored graphs Γ' such with $|\mathrm{sp}_1 \Gamma'| \geqslant 53$ and $|\mathrm{sp}_0 \Gamma'| \neq 0$,

where $\mathrm{sp}_j \Gamma'$ stands for the induced subgraph of Γ' given by all its vertices of color $j = 0, 1$. Moreover, by (7.3), the (plain) graph $\Gamma := \mathrm{sp}_1 \Gamma'$ is a Σ-graph for a certain affine Dynkin diagram $\Sigma \geqslant \tilde{\mathbf{A}}_2$.

The monotonicity given by [2, Lemma 2.8] combined with the consideration of §6 implies that the graph Γ is neither pentagonal (see Proposition 6.2), nor astral (see Proposition 6.4), nor locally elliptic (see (6.5)). Finally, Proposition 5.6 shows that

$$\Gamma \text{ is triangular.}$$

Then, by Lemma 3.11 and Proposition 3.12, we necessarily have $\mathrm{rk}(\Gamma) = 20$, upon which Addendum 3.23 implies that Γ is one of the eight smooth configurations found in [8]. For each graph Γ obtained we compute its extended saturation(s) $\mathrm{sat}^{\mathrm{ex}}\,\Gamma$ and check that none of the resulting bi-colored graphs has a vertex of color zero (exceptional divisor), completing the proof of Theorem 1.1. $\qquad\square$

7.3. **Proof of Theorem 1.2.** When dealing with smooth quartics, we can confine ourselves to the case where the lattice $\mathrm{NS}(X_4)$ is spanned by lines, see Remark 7.5 and (4.2). Theorem 7.4 reduces the proof to the classification of all graphs Γ such that

$$\Gamma \text{ is geometric and } |\Gamma| \geqslant 49;$$

then, by (7.3), the (plain) graph Γ is a Σ-graph for a certain affine Dynkin diagram $\Sigma \geqslant \tilde{\mathbf{A}}_2$. As in the proof of Theorem 1.1, we infer that Γ is neither quadrangular (Proposition 5.6), nor pentagonal (Proposition 6.2), nor astral (Proposition 6.4), nor locally elliptic (see (6.5)).

For a geometric triangular graph Γ with at least 49 vertices and $\mathrm{rk}(\Gamma) < 20$, we apply Proposition 4.8 to show that Γ is one of the five graphs (4.9). Otherwise, by Addendum 4.10, the graph Γ is one of the rank 20 graphs that appear in Table 1.

To complete the deformation classification, let Γ be one of the graphs in Table 1. As part of our study of the saturation lists, we observe that the only geometric finite index extension of $\mathcal{F}(\Gamma)$ is the trivial one; hence, one has

$$(7.9) \qquad \mathrm{NS}(X_4) = \mathcal{F}(\Gamma) \quad \text{and} \quad O_h(\mathrm{NS}(X_4)) = \mathrm{Aut}\,\Gamma$$

for any smooth quartic $X_4 \subset \mathbb{P}^2$ with $\mathrm{Fn}\,X_4 \cong \Gamma$, and the latter group is found using the digraph package in GAP [9]. According to [8, Theorem 3.9], the equilinear deformation families of such quartics are in a bijection with the primitive isometric embeddings

$$(7.10) \qquad S := \mathcal{F}(\Gamma) \hookrightarrow \mathbf{L} = 2\mathbf{E}_8 \oplus 3\mathbf{U}$$

regarded up to polarized autoisometry of $S \ni h$ and autoisometry of $\mathbf{L}$ preserving a coherent orientation of maximal positive definite subspaces of $\mathbf{L} \otimes \mathbb{R}$ (the so-called *positive sign structure*); such a family is real if and only if (7.10) admits a polarized autoisometry reversing the positive sign structure. Hence, to complete the proof, we classify embeddings (7.10) using Nikulin's [16] theory of discriminant forms and either Gauss [10] theory of binary quadratic forms (in the definite case $\mathrm{rk}\,T = 2$) or Miranda–Morrison [13] theory (in the indefinite case $\mathrm{rk}\,T \geqslant 3$). $\qquad\square$

Remark 7.11. The groups $\mathrm{Sym}\,X_4$ and $\mathrm{Aut}(X_4, h)$ in Table 1 are computed as the subgroups of (7.9) that, respectively, act identically on $\mathrm{discr}\,S$ or extend to an appropriate autoisometry of $\mathbf{L}$: the latter is required to preserve the positive sign structure (if $\mathrm{rk}\,T = 2$) or act on T by ± 1 (if $\mathrm{rk}\,T \geqslant 3$).

7.4. **Proof of Addendum 1.3.** As stated in [8, Addendum 1.4], the number of real lines does take all values in the range $\{0, \ldots, 48\}$. Next, we recall that, when counting the number of real lines on *smooth* quartics, it suffices to consider only those quartics X_4 whose *all* lines are real (with respect to a certain real structure $\sigma\colon X_4 \to X_4$, see [8, Proposition 3.10] or [5, Theorem 2.7]), and the latter is the case if and only if the generic transcendental lattice T has a sublattice isomorphic to [2] or $\mathbf{U}(2)$, see [8, Lemma 3.8]. Hence, the statement of the addendum follows from Table 1 which lists all configurations of more than 48 lines and their respective transcendental lattices. □

References

1. J. H. Conway and N. J. A. Sloane, *Sphere packings, lattices and groups*, Grundlehren der Mathematischen Wissenschaften [Fundamental Principles of Mathematical Sciences], vol. 290, Springer-Verlag, New York, 1988, With contributions by E. Bannai, J. Leech, S. P. Norton, A. M. Odlyzko, R. A. Parker, L. Queen and B. B. Venkov. MR 920369 (89a:11067)

2. A. Degtyarev and S. Rams, *Counting lines with Vinberg's algorithm*, 2021, To appear, arXiv:2104.04583.

3. _____, *Lines on $K3$-sextics*, in preparation, 2021.

4. _____, *Ancillary files for the paper: Lines on $K3$-quartics via triangular sets*, 2022, available on the arXiv as ancillary files for this preprint.

5. Alex Degtyarev, *Lines on Smooth Polarized K3-Surfaces*, Discrete Comput. Geom. **62** (2019), no. 3, 601–648. MR 3996938

6. _____, *Smooth models of singular K3-surfaces*, Rev. Mat. Iberoam. **35** (2019), no. 1, 125–172. MR 3914542

7. _____, *Lines in supersingular quartics*, J. Math. Soc. Japan **74** (2022), no. 3, 973–1019. MR 4484237

8. Alex Degtyarev, Ilia Itenberg, and Ali Sinan Sertöz, *Lines on quartic surfaces*, Math. Ann. **368** (2017), no. 1-2, 753–809. MR 3651588

9. *GAP – Groups, Algorithms, and Programming, Version 4.10.1*, https://www.gap-system.org, Feb 2019.

10. Carl Friedrich Gauss, *Disquisitiones arithmeticae*, Springer-Verlag, New York, 1986, Translated and with a preface by Arthur A. Clarke, Revised by William C. Waterhouse, Cornelius Greither and A. W. Grootendorst and with a preface by Waterhouse. MR 837656 (87f:01105)

11. Víctor González-Alonso and Sławomir Rams, *Counting lines on quartic surfaces*, Taiwanese J. Math. **20** (2016), no. 4, 769–785. MR 3535673

12. C.M. Jessop, *Quartic surfaces with singular points*, Cambridge University Press, Cambridge, 1916.

13. Rick Miranda and David R. Morrison, *Embeddings of integral quadratic forms*, Electronic, http://www.math.ucsb.edu/~drm/manuscripts/eiqf.pdf, 2009.

14. Yoichi Miyaoka, *Counting lines and conics on a surface*, Publ. Res. Inst. Math. Sci. **45** (2009), no. 3, 919–923. MR 2569571

15. V. V. Nikulin, *Finite groups of automorphisms of Kählerian K3 surfaces*, Trudy Moskov. Mat. Obshch. **38** (1979), 75–137. MR 544937

16. _____, *Integer symmetric bilinear forms and some of their geometric applications*, Izv. Akad. Nauk SSSR Ser. Mat. **43** (1979), no. 1, 111–177, 238, English translation: Math USSR-Izv. 14 (1979), no. 1, 103–167 (1980). MR 525944 (80j:10031)

17. Sławomir Rams and Matthias Schütt, *112 lines on smooth quartic surfaces (characteristic 3)*, Q. J. Math. **66** (2015), no. 3, 941–951. MR 3396099

18. _____, *64 lines on smooth quartic surfaces*, Math. Ann. **362** (2015), no. 1-2, 679–698. MR 3343894

19. B. Saint-Donat, *Projective models of K-3 surfaces*, Amer. J. Math. **96** (1974), 602–639. MR 0364263 (51 #518)

20. B. Segre, *The maximum number of lines lying on a quartic surface*, Quart. J. Math., Oxford Ser. **14** (1943), 86–96. MR 0010431 (6,16g)

21. Ichiro Shimada, *Connected components of the moduli of elliptic K3 surfaces*, Michigan Math. J. **67** (2018), no. 3, 511–559. MR 3835563

22. Davide Cesare Veniani, *Lines on K3 quartic surfaces in characteristic 2*, Q. J. Math. **68** (2017), no. 2, 551–581. MR 3667213
23. _____, *The maximum number of lines lying on a K3 quartic surface*, Math. Z. **285** (2017), no. 3-4, 1141–1166. MR 3623744
24. _____, *Symmetries and equations of smooth quartic surfaces with many lines*, Rev. Mat. Iberoam. **36** (2020), no. 1, 233–256. MR 4061988
25. _____, *Lines on K3 quartic surfaces in characteristic 3*, Manuscripta Math. **167** (2022), no. 3-4, 675–701. MR 4385387

Department of Mathematics, Bilkent University, 06800 Ankara, TURKEY
Email address: degt@fen.bilkent.edu.tr

Institute of Mathematics, Jagiellonian University, ul. Łojasiewicza 6, 30-348 Kraków, Poland
Email address: slawomir.rams@uj.edu.pl